

Cite this article as: Wang Cuiping, Zhang Huan, Wu Guoqiang, et al. One-Pot Preparation of Gold Porous Nanoplates and Their Application in SERS Detection[J]. Rare Metal Materials and Engineering, 2022, 51(10): 3655-3662.

ARTICLE

One-Pot Preparation of Gold Porous Nanoplates and Their Application in SERS Detection

Wang Cuiping, Zhang Huan, Wu Guoqiang, Hong Yanping, Yan Xianzai, Yu Lili, Wang Chunrong

School of Food Science & Engineering, Jiangxi Agricultural University, Nanchang 330045, China

Abstract: Design and fabrication of various gold micro- and nanostructures is a promising way to amplify surface enhanced Raman scattering (SERS) signals. Gold porous nanoplates were produced by simple heating aqueous solutions of HAuCl_4 and polyethylene glycol (PEG). The reaction was carried out in a one-pot, by one-step process at mild temperature, and PEG was used as capping agent and reducing agent in this cost-effective and environmentally benign fabrication strategy. Results show that the gold porous plates are about several micrometers in size and can be modified by experimental parameters such as growth time, PEG concentration, and gold ion concentration. The EDS measurements confirm the metallic nature of the cleaned gold porous nanoplates with no organic contaminants on the surface. The gold porous nanoplate substrate offers an excellent SERS-effect and exhibits a good reproducibility in SERS detection. Importantly, the as prepared gold porous plate substrates can be used for rapid and highly sensitive determination of organic pesticides such as thiram and phorate.

Key words: gold; porous nanoplates; SERS; polyethylene glycol

Noble metallic nanostructures exhibit a phenomenon known as surface-enhanced Raman scattering (SERS) in which the weak intensity of normal Raman spectroscopy is tremendously improved through adsorbing target molecules onto metal surfaces^[1]. SERS can provide rich structural and molecular fingerprints up to trace levels, and has proven to be a powerful tool in the field of environmental protection and food safety^[2,3]. Importantly, the special morphology and size of metal particles are prerequisites for stronger SERS enhancement, due to the existence of so-called “hot spots” having intense local electromagnetic fields in which highly efficient Raman scattering can be obtained^[4].

Gold (Au), as one of the most common noble metals, has often considered as an excellent candidate for SERS substrates^[5]. Until now, a large number of various anisotropic gold nanostructures including nanoplates^[6], nanowires^[7], nanoflowers^[8] and other hierarchical nanoarchitecture^[9] have been proven to be effective as SERS substrates for the signal amplification. Among them, gold porous structures have attracted much interest because their porous surface can afford

lots of “hot spots”, which facilitate the acquisition of better Raman peaks^[4]. Therefore, extensive efforts have been devoted to search for novel methods for the preparation of gold porous structures, for example, de-alloying^[10] electrochemical deposition^[11], templated electrochemical deposition^[12], sputter^[13], and spray deposition^[14]. Unfortunately, all these above-mentioned approaches suffer from more or less unacceptable shortcomings such as requiring complex preparation process, specialized equipment, high cost, non-environmentally-friendly technology, and easily being contaminated with organics, which push the scientist to explore new alternative solutions to overcome such limitations.

In this study, a facile, environmentally benign one-step approach was developed to obtain gold porous nanoplates in high yields. This porous nanoplates were synthesized by adding PEG and chloroauric acid in aqueous solutions. The resulting gold porous nanoplates were about several micrometers in size, and there were a large number of irregular pores with the size of tens of nanometers on the surface. The porous plates can be reproducibly produced with

Received date: October 13, 2021

Foundation item: National Natural Science Foundation of China (31960500); Science and Technology Project of Education Department of Jiangxi Province (170282)
Corresponding author: Wang Chunrong, Ph. D., Professor, School of Food Science and Engineering, Jiangxi Agricultural University, Nanchang 330045, P. R. China, Tel: 0086-791-83813420, E-mail: crwang2017@jxau.edu.cn

Copyright © 2022, Northwest Institute for Nonferrous Metal Research. Published by Science Press. All rights reserved.

high yields. No organic contaminants were found on the surface of the porous plates. The influence of experimental parameters including PEG concentration, chloroauric acid concentration, and the reaction time on the porous plate formation was also examined. It was also found that the morphology is critical for the SERS performance. The prepared gold porous nanoplate substrates were successfully employed for detecting anthracene, 4-mercaptopyridine, thiram and phorate, indicating that they have a good future for implementation.

1 Experiment

1.1 Materials

Analytical standard grade thiram (99.9%), phorate (99.5%), 4-mercaptopyridine (4-Mpy, 99.5%), anthracene ($\geq 99.7\%$), polyethylene glycol (PEG 10000), $\text{HAuCl}_4 \cdot 3\text{H}_2\text{O}$ (99.9%), and sodium chloride (99.5%), potassium dichromate ($\geq 99.8\%$), sulfuric acid (95.0% to 98.0%), hydrochloric acid (34% to 37.5%), acetone ($\geq 99.5\%$), ethanol (100%), and methanol (99.9%) were procured from Aladdin Reagent Co., Ltd (Shanghai, China).

1.2 Preparation of porous gold nanoplates

Briefly, 100 mL of HAuCl_4 solution (0.8 mmol/L) was slowly added to 100 mL of aqueous PEG (0.2 mmol/L) in a beaker under stirring. After the reaction solution was kept at 50 ± 0.5 °C for 24 h, gold porous nanoplates were formed and collected. Then, the prepared gold porous nanoplates were soaked in the newly prepared chromic acid and washed with deionized water to remove PEG. The clean gold porous nanoplates were stored in deionized water and then sealed for further tests.

The morphology of porous gold nanoplate and SERS substrate was evaluated by scanning electron microscope (SEM), high-resolution transmission electron microscopy (TEM), EDS spectrum, X-ray diffraction (XRD), and ultraviolet-visible-near infrared absorption spectra (UV-vis-NIR). The SEM images and EDS spectrum were observed by a JSM-6700F field emission scanning electron microscopy (JEOL Ltd., Japan) operated at 3.0 kV. TEM images were obtained using a JEM-2010 emission transmission electron microscopy (JEOL Ltd, Japan) at accelerating voltages of 200 kV. X-ray diffraction (XRD) data were taken from a D8 Advance X-ray diffractometer (Bruker AXS Ltd., Germany) with Cu K α radiation ($\lambda = 0.154$ 06 nm). Finally, the solutions were analyzed by a SPECORD 200 PLUS ultraviolet visible spectrophotometer (Analytik Jena AG Ltd, Germany).

1.3 SERS detection and data analysis

The as-prepared porous gold nanoplates were used as SERS-active substrates. Anthracene was chosen as model analytes to investigate the performance of the porous gold nanoplates-based substrate. 4-Mpy was chosen for the relative standard deviation (RSD) analysis. Thiram and phorate was used for the limit detection (LOD) and the limit of quantitation (LOQ) detection. Typically, 2 μL of working standard solutions of thiram (different concentrations from 0.5

mg/L to 10 mg/L) was dropped on a piece of parafilm (1 cm \times 1 cm). After that, 2 μL of gold porous nanoplates (~ 250 $\mu\text{g}/\text{mL}$) was added and mixed by pipetting for 20 s, and then 2 μL of the mixture was transferred onto the glass slide, and dried by nitrogen-blowing for Raman measurement.

A DXR Raman microscope (Thermo Fisher Scientific, USA) with a 780 nm laser and a 50 \times confocal microscope objective (0.8 mm spot diameter and 2 cm $^{-1}$ spectral resolution) was used to carry out the SERS measurements. Each spectrum was scanned with 2 mW laser power and a 25-mm slit width for 2 s integration time. OMNIC software version 9.0 (Thermo Fisher Scientific) was used to control the Raman instrument.

The limits of detection (LOD) and the limit of quantitation (LOQ)^[15] for thiram and phorate were tested on blank samples ($n = 6$) using the following standard equation:

$$\text{LOD} = 3S_b/M \quad (1)$$

where S_b is the standard deviation of the SERS intensity of the blank at Raman shifts of 1380 cm $^{-1}$ for thiram and 635 cm $^{-1}$ for phorate, and M represents the slope of plotted calibration curves. The limit of quantitation was calculated by

$$\text{LOQ} = 10S_b/M \quad (2)$$

Moreover, linear calibration curves were used to calculate the linear correlation between the SERS intensity of characteristic peaks and various concentrations of thiram and phorate in standard solutions.

2 Results and Discussion

2.1 Characteristic of gold porous nanoplates

The morphology of as-prepared products was characterized by scanning electron microscopy and high-resolution transmission electron microscopy (Fig. 1a–1c). The SEM image shows that there are a large number of gold porous nanoplates with a diameter of about 5 μm (Fig. 1a). These nanoplates were cleaned using chromic acid before TEM detection, in order to eliminate the influence of organic pollutants. It is well established that the color of organic matter such as PEG is much lighter than that of metal material, and often gray and fuzzy in the field of electron microscope^[16]. In Fig. 1b, these possible organic are not found at the edge of the nanoplates, which suggests that the gold nanoparticles are relatively clean after chromic acid treatment. Enlarged TEM images show that there are a large number of ternary or irregular pores with diameters ranging from a few nanometers to tens of nanometers that are distributed on the gold nanoplates (Fig. 1c). Among all the pore size distributions, about 70% of the pores have size less than 5 nm, 15.7% are 5–10 nm, and 14.3% are 10–20 nm. Interestingly, closer inspection of TEM of the porous plate allows the direct visualization of fold structures, which may come from interface dislocations. The origin of these defects is likely a consequence of the growing mechanism itself. When crystals are formed by coalescence of grains at crystallographically specific surfaces, a small misorientation at the interface can result in dislocations^[17].

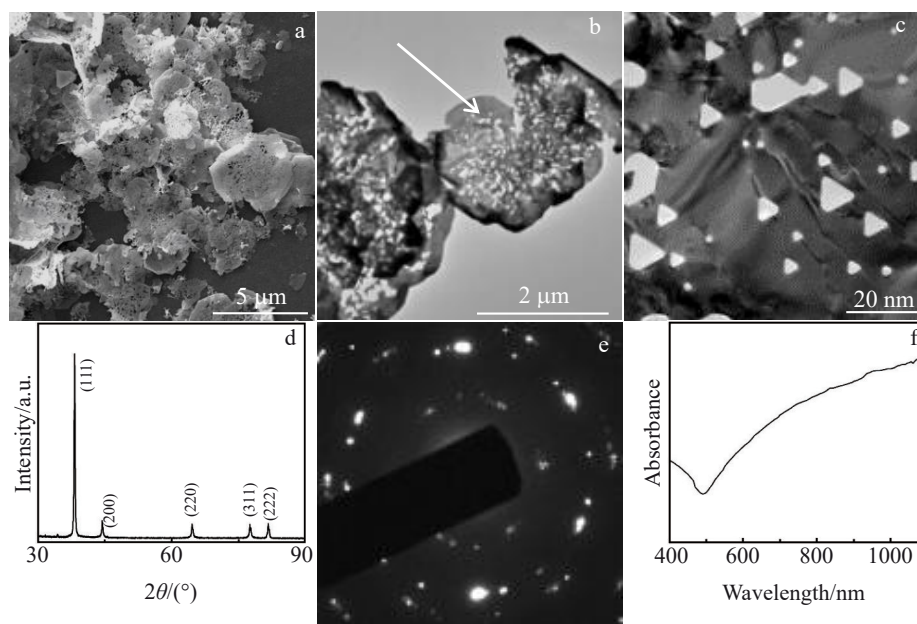


Fig.1 SEM images of gold porous nanoplates not cleaned (a) and cleaned with chromic acid (b); enlarged TEM image of the porous nanoplate marked by arrow in Fig. 1b (c); XRD pattern (d); SAED pattern of single gold porous nanoplate in Fig. 1b (e); UV-vis-NIR absorbance spectrum of gold porous nanoplates solution (f) (concentrations of PEG and HAuCl_4 are 0.1 and 0.4 mmol/L, respectively)

The XRD pattern (Fig. 1d) proves the expected diffraction peak of fcc structure of gold. However, the intensity ratios of (111) and (200) diffraction peaks are much higher than the normal intensity ratio. This feature is a characteristic of thin structures primarily bound by {111} facets with a high tendency to be oriented parallel to the substrate^[18]. Selected area electron diffraction (SAED) analysis carried out by focusing the beam on a whole structure (Fig. 1c) shows a pattern that is indexed based on the fcc structure of gold. The SAED pattern is not consistent with a perfect single-crystal or polycrystalline structure. The presence of additional spots indicating slight misorientation between different inner zones of plate, which may be several branches joined to form a network^[17,19]. Therefore, the gold porous plate may be a structure between single crystal and polycrystal^[19,20]. This result is verified with the interface dislocations in Fig. 1c. The product reaction solution has strong absorption in the near infrared region (Fig. 1f), which also proves that large-scale gold nanostructures are formed^[21].

The chemical compositions of the cleaned gold porous nanoplates deposited on the glass slide were confirmed with the energy-dispersive spectrometry (EDS). As an example, the EDS spectrum obtained from Fig. 2a reveals the presence of Au and Si, Na and O elements (Fig. 2b). The peaks of Si, Na and O originate from glass substrate. Although there may be a small number of residual PEG molecules adsorbed on gold nanostructures, trace of carbon (from PEG molecules) is not detected, which demonstrates that a majority of PEG molecules have been washed off the solid substrates. Therefore, the products are pure metallic gold^[22].

To gain insight into the possible growth mechanism, the time evolution of the porous plate structures during the

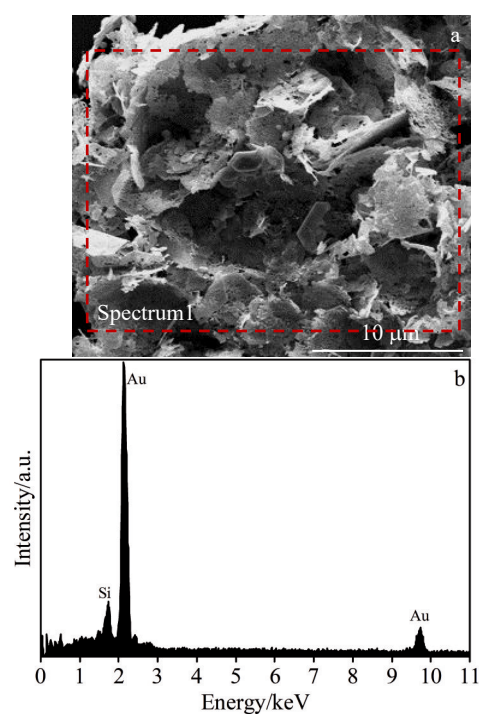


Fig.2 SEM image of the as-prepared gold porous nanoplates cleaned with chromic acid (a) and EDS spectrum of the selected area marked in Fig. 2a (b)

synthesis was investigated by TEM, SEM and UV-vis spectrophotometry. Fig. 3 shows TEM, SEM images and UV-vis-NIR spectra of the samples with varying reaction durations (from 0.5 h to 24 h), while keeping other parameters exactly the same. TEM observation of the product heated for

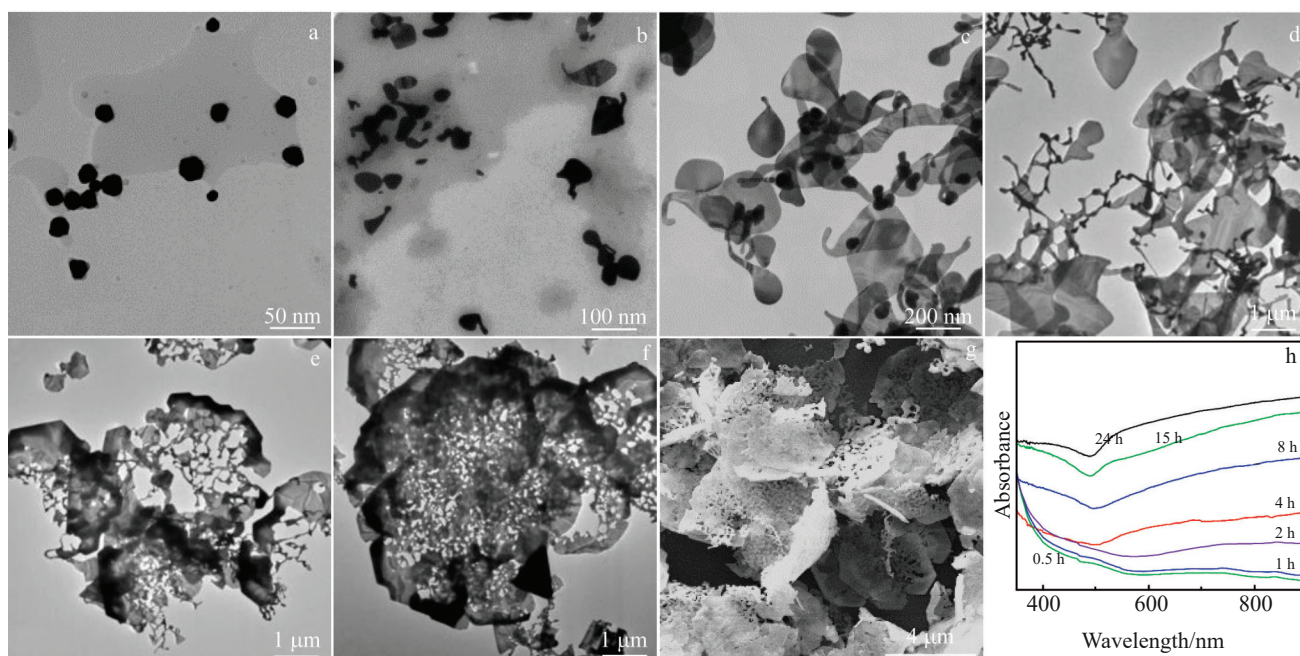


Fig.3 TEM images of gold nanostructures formed with different reaction time of 0.5 h (a), 1 h (b), 2 h (c), 4 h (d), 8 h (e) and 15 h (f) after the mixing of PEG and HAuCl_4 aqueous solution; SEM image of gold porous nanoplates obtained after 24 h (g); UV-vis-NIR absorbance spectra of reacted solution (h)

only 0.5 h reveals that gold spherical nanoparticles with diameter in the range of 20~50 nm are randomly scattered in the reacted solution (Fig. 3a). The UV-vis spectra also prove that a low amount of metal particles are obtained in this short reaction time (Fig. 3h). With increasing the reaction time to 1 h, the size of the gold cluster becomes obviously larger, showing increased reduction for HAuCl_4 (Fig. 3b). Besides spherical gold nanoparticles, some branched gold units are also observed. The growth of branched structures by extending the reaction time to 2 h is clearly seen from TEM image (Fig. 3c), and two-dimensional tadpole shaped gold nanoparticles with a length more than 200 nm are generated. The products obtained after reaction for 4 and 8 h are shown in Fig. 3d and Fig. 3e, respectively, where the branched gold structures are connected in a network structure and the discrete nanoparticles are decreased evidently. After 15 h of growth (Fig. 3f), porous plates with diameter more than 4 μm appear in the reacted solution. Both TEM and UV-vis analysis indicate that the formation of the porous plate structures starts with the aggregation of small gold units formed by reduction of the metal salt (Fig. 3). When the reaction time is further increased to 24 h, a large number of gold porous plates are synthesized, and no evident difference of morphology is observed compared to the products with 15 h reaction time. It should be noted that the resulting gold porous plates remains unchanged after a washing process, which indicates that these products have satisfactory stability as SERS substrate. Besides, the reactions are carried out at 50 °C, indicating that the formation of gold porous nanoplates is a mild process. TEM, SEM and UV-vis analysis indicates that formation of the porous plate structures starts with the aggregation of small

gold nanostructure units formed by reduction of the metal salt. The nature of these gold nanostructure units in the initial stage and reaction will be influenced by the slow reaction rate^[23].

It is well established that a low global concentration of polymer is crucial for the development of branched structures^[19]. Fig. 4 shows SEM, TEM images of the Au nanostructures and SERS spectra with varying the concentration of PEG from 0.1 mmol/L to 2.4 mmol/L while keeping a constant concentration of 0.4 mmol/L AuCl_4^- . SEM and TEM images in Fig. 4 show that the nanostructures change from porous plate (Fig. 4a) to branched structure (Fig. 4b~4d) and sphere with a few triangular plates (Fig. 4e) with the increase of PEG concentration. It is worth noting that the gold porous plates offer the most significant enhancement effect on the Raman spectrum among these nanostructures in Fig. 4f. The experimental results clearly show that synthesis of porous plates is favored in conditions of high dilution PEG.

In addition, the gold ions with higher concentration have been reported to improve the fusion of gold particles^[24]. As shown in Fig. 5, the TEM images reveal that the hole density of products increase as the increase of HAuCl_4 concentration (from 0.05 mmol/L to 0.5 mmol/L). In these reacted solutions, gold nanoparticles may hit and stick together randomly, followed by deposition of newly formed gold atoms onto surfaces of nanoparticles and the concave region of the connected particles, according to hit-to-stick-to-fusion model^[25]. Although a low supersaturation of gold atoms may enhance the development of open, extended structures with a branched appearance, gold nanoparticles in high concentration easily aggregated together can increase hole density on gold plate and thereby the number of "hot spots". This conjecture

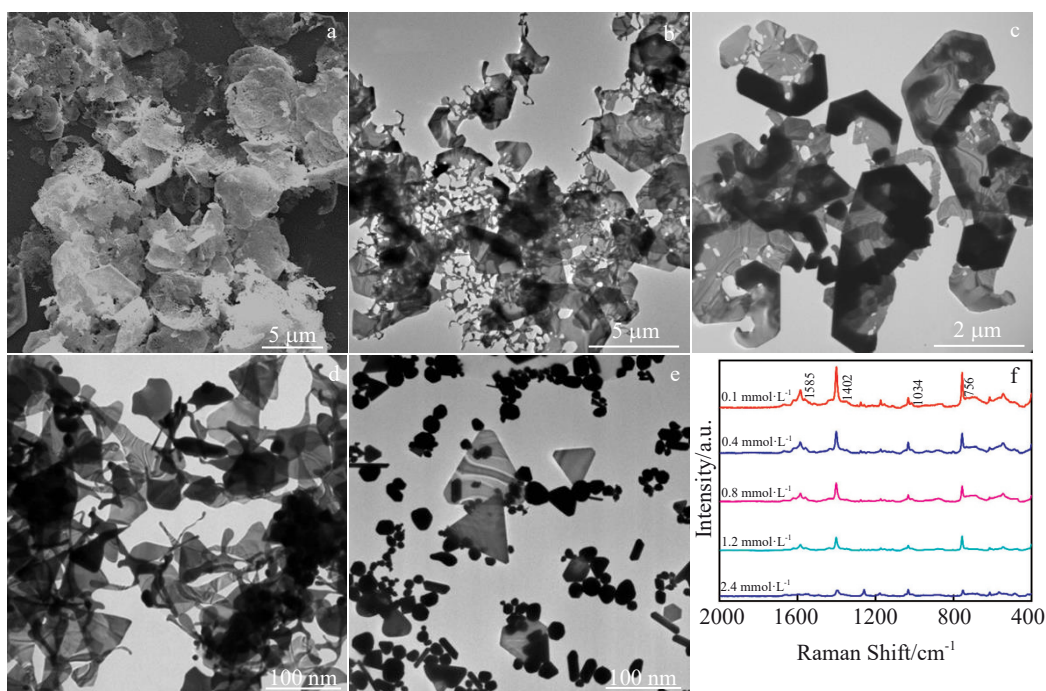


Fig.4 SEM (a~c) and TEM (d, e) images of Au nanostructures formed under different PEG concentrations: (a) 0.1 mmol/L, (b) 0.4 mmol/L, (c) 0.8 mmol/L, (d) 1.2 mmol/L, and (e) 2.4 mmol/L; (f) corresponding SERS spectra of anthracene analyte based on different gold nanostructures prepared under corresponding PEG concentrations of Fig.4a~4e (concentration of AuCl_4^- is 0.4 mmol/L)

is confirmed by SERS experimental results (Fig.5e).

2.2 Growth mechanism

Based on the above investigations, our findings point toward a mechanism in which morphology of gold nano-

structures might be controlled by gold atom supersaturation and protection efficiency against aggregation at mild temperature^[26,27]. Moreover, final structures can be explained based on hit-to-stick-to-fusion model^[25] and expedite preferential

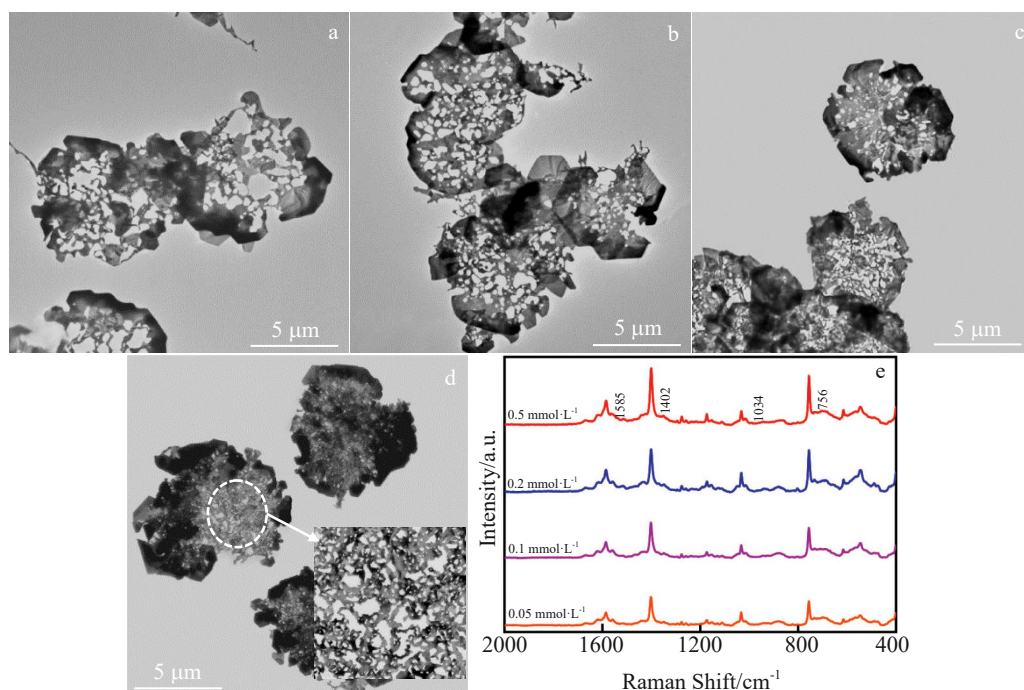


Fig.5 TEM images of gold nanostructures obtained at different HAuCl_4 concentrations: (a) 0.05 mmol/L, (b) 0.1 mmol/L, (c) 0.2 mmol/L and (d) 0.5 mmol/L; SERS spectra of anthracene analyte based on porous gold nanoplates prepared under different HAuCl_4 concentrations (e) (concentration of PEG is 0.1 mmol/L)

growth along the oriented directions due to inefficient protection^[19,26]. The presence of tiny irregular holes, as well as dimples and dislocations, is a very common feature of these structures^[17,19]. Unraveling of the detailed mechanism will certainly require further investigation; however, a possible explanation for the presence of these structural characteristics is that the growth of gold porous nanoplate may go through three main stages. First, a portion of AuCl_4^- is reduced to form gold nanoparticles at the initial reaction stage (Fig. 3a), in which PEG not only acts as a reducing agent but also a capping agent in the reduction reaction^[28]. Compared with the reactions at high temperature (100 °C) in the traditional hydrothermal synthesis method^[29], the temperature in our preparation method is mild (50±0.5 °C). Therefore, PEG may substantially slow down the hydrothermal reaction rate to produce a few gold particle seeds at mild temperature, thanks to its weak reducing power^[30]. Second, as reported by Lin et al.^[31], the slow reaction rate triggers the kinetic control regime for crystal growth to render the formation of thermodynamically unfavorable shape. PEG, preferentially bound to {111} facets of Au^[27,32], will expedite preferential growth along the lateral directions, leading to two-dimensional anisotropic growth to cause branched nanostructure units or network structure formation (Fig. 3b, Fig. 3c and Fig. 5d)^[19]. An oriented attachment process (OA) involves spontaneous self-organization of adjacent particles so that they share a common crystallographic orientation (Fig. 1e)^[33], followed by joining of these particles at a planar interface which are essentially unstable and thus inclined to be attached by the feed atoms^[34]. In this process, formation of dislocations due to a small misorientation in the interface is common, as well as the presence of dimples and other defects. The van der Waals attractive interaction between the gold surfaces results in the attractive interaction among gold nanoparticles, which acts as driving factors for the fusing process^[35]. However, gold nanoparticles will be more closely protected when there are too much PEG in the reacted solution, and the possibility of gold nanoparticles to become a multi-branched structure will be reduced (Fig. 4). In extreme cases, only spherical gold nanoparticles will be formed in the reaction solution even in the presence of excess PEG. Third, the anisotropic coalescence of these branched or non-branched nanostructures forms the nanowire networks^[36] which further grow into a nearly circular porous plates (Fig. 3d~3g). In the last reacted process, high concentration of gold ions will help to improve the density of holes of porous plate according to hit-to-stick-to-fusion growth process^[37]. Obviously, too much gold ions may also lead to the disappearance of small holes and the formation of solid sheet structure. This will be discussed in our future research. The above assumptions are consistent with the XRD, ED, TEM and SEM analyses of gold porous nanoplates in our experiment. Hence, our findings point toward a possible mechanism in which synthesis of porous structures is favored in conditions of low neutral polymer, high HAuCl_4 and mild reaction rates. The use of a neutral polymer with low protection efficiencies for the particles

possibly plays an important role in this process of fabrication of metal porous structures while simultaneously avoiding fast precipitation of the products. It is worth noting that our preparation method of gold porous nanoplates has obvious advantages compared with the traditional method. This method is one-step synthesis without adding template and easy to operate. The pore size distribution of gold porous nanoplates can be easily controlled by adjusting the content of PEG and HAuCl_4 . It is of great value for the further development and practical application of gold porous nanoplates.

2.3 SERS properties

A common problem with the SERS substrate is the reproducibility (substrate uniformity) of the as-prepared gold porous nanoplates^[38]. In this study, SERS spectra of 4-MPy were collected from 12 random-selected sites on the same substrate under the same experimental conditions. The result (Fig. 6) shows a satisfactory consistency of the SERS performance detected on the same substrates. For the strongest peak (ring breathing modes^[39]) at 1005 cm^{-1} , the relative standard deviation (RSD) of the SERS intensity is about 8.41%. In addition, SERS spectra of 4-MPy from randomly selected 12 SERS substrates from the same batch were also detected, and the experimental results are similar, with an RSD of about 8.55%. The above research results indicate that the gold porous nanoplates are rather potential for the sensitive and reproducible SERS sensing^[29].

In recent years, food safety issues, especially pesticide residues in food, have received increasing attention^[40]. As shown in Fig. 7, the as-prepared SERS-active gold porous plate substrates are employed for the sensitive and rapid detection of pesticides of thiram and phorate. In Fig. 7a, thiram at various concentrations (0.5~500 $\mu\text{g/L}$) in water (Fig. 7a) was detected by drop method. Although the background fluorescence interference is observed, the main characteristic peaks of 554, 1145, 1380 and 1509 cm^{-1} are depicted clearly in the SERS spectra, even in the spectrum from sample with as

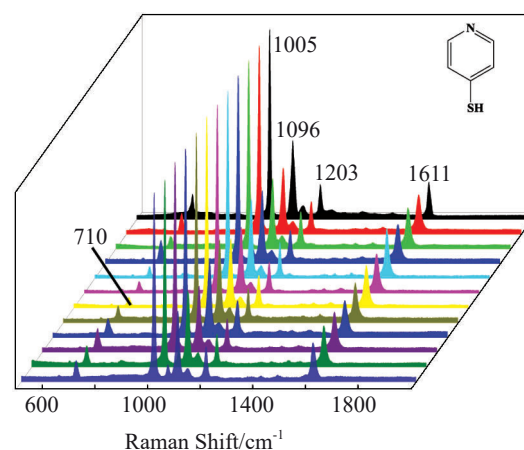


Fig.6 SERS spectra of 4-MPy analyte collected from 12 random sites on the as-prepared gold porous nanoplates of one SERS substrate

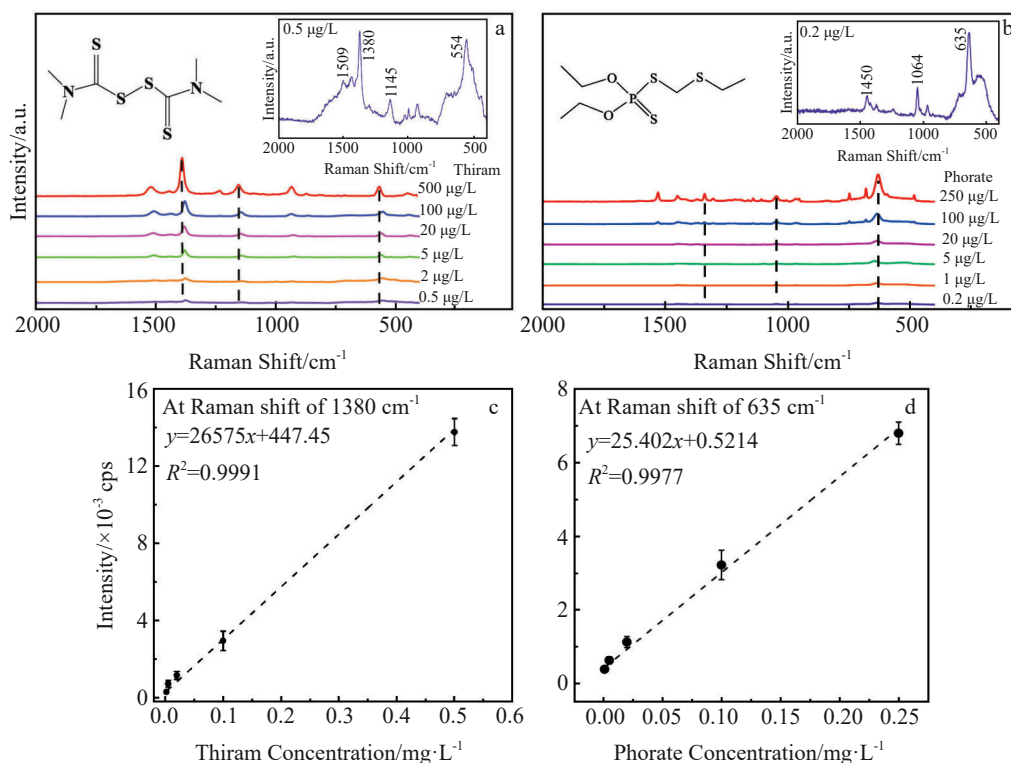


Fig.7 Raman spectra of thiram (a) and phorate (b) in water; calibration curves in thiram (c) and phorate (d) of the gold porous nanoplates

low as 0.5 $\mu\text{g/L}$ thiram (inset in Fig. 7a). These characteristic Raman bands are assigned to thiram's unique Raman scattering^[41]. Obviously, the lowest detectable concentration of thiram may be far lower than 0.5 $\mu\text{g/L}$ according to these clear characteristic peaks in Fig. 7a. Thiram concentration and Raman intensity present a nice linear relation with coefficient of determination (R^2) of 0.9991. The limit of detection (LOD) value is calculated to be 0.53 $\mu\text{g/L}$, which is confirmed by the detection of 0.5 $\mu\text{g/L}$ thiram in Fig. 7a. The theoretical limit of quantification value can be extended to 1.76 $\mu\text{g/L}$ using Eq. (2). These values are far lower than the reported value of 36.7 $\mu\text{g/L}$ ^[41]. When the thiram concentration is as low as 0.005 $\mu\text{g/L}$, resolvable signals can still be detected at the Raman characteristic peaks. For phorate, the main characteristic peaks are 635, 1064 and 1450 cm^{-1} ^[42]; the coefficient of determination (R^2) is 0.9977; LOD and LOQ are calculated to be 0.21 $\mu\text{g/L}$ and 0.70 in water, respectively. As the phorate concentration is as low as 0.002 $\mu\text{g/L}$, clear signals can still be detected at the Raman characteristic peaks. These results are obviously better than other SERS methods reported, which are 10 and 50 $\mu\text{g/L}$ ^[42,43]. The detection limit of this method is lower than that of other reported SERS detection results, and far lower than the requirements for the maximum residues of thiram (0.1 mg/L) and phorate (0.01 mg/L) in GB2763-2021^[44]. It has a good application prospect in the rapid detection of practical products.

3 Conclusions

1) A simple one-step environmentally friendly route is

developed for the synthesis of gold porous plates by adding HAuCl_4 and PEG in aqueous solutions at mild temperature. The porous morphology is critical for the SERS enhancement. This synthesis method is promising to be extended to the synthesis of various noble metal nanomaterials with multi-branched structures.

2) EDS measurements demonstrate the metallic nature of the formed gold porous plates. The as-prepared gold porous plates, as SERS substrates, exhibit a good reproducibility for SERS detection, with a relative standard deviation of 8.4%.

3) Compared with the products by traditional SERS methods, the as-prepared gold porous SERS-active substrates has improved sensitivity in detecting organic compounds such as thiram and phorate, which indicates a promising application in rapid chemical analysis areas.

References

- 1 Zhang R, Olin H K. *Materials*[J], 2014, 7(5): 3834
- 2 Zhou Z, Lu J, Wang J et al. *Spectrochimica Acta Part A: Molecular and Biomolecular Spectroscopy*[J], 2020, 234: 118 250
- 3 Asgari S, Wu G, Aghvami S A et al. *Food Additives & Contaminants: Part A*[J], 2021, 38(4): 646
- 4 Lim D, Jeon K, Kim H M et al. *Nature Materials* [J], 2010, 9(1): 60
- 5 Manisekaran R, Jiménez-Cervantes Amieva E, Valdemar-Aguilar C M et al. *Gold Bulletin*[J], 2020, 53(3): 135
- 6 Peng Y, Yu L, Lu X et al. *Journal of Materials Chemistry B*[J],

- 2018, 6(21): 2813
- 7 He Y, Chen Y, Xu Q et al. *ACS Appl Mater Inter*[J], 2017, 9(8): 7826
- 8 Osminkina L A, Žukovskaja O, Agafilushkina S N et al. *Applied Surface Science*[J], 2020, 507: 144 989
- 9 Li H, Dai H, Zhang Y et al. *Nano Energy*[J], 2019, 64: 103 959
- 10 Xue Y, Paschalidou E M, Rizzi P et al. *Philosophical Magazine* [J], 2018, 98(30): 1
- 11 Martynova N A, Goldt A E, Maslakov K I et al. *Journal of Materials Science*[J], 2018, 53(11): 7953
- 12 Khalil I, Chou C, Tsai K et al. *Applied Sciences*[J], 2019, 9(22): 4806
- 13 Matthias S, Adeline B, Volker K et al. *Nanoscale*[J], 2013, 5(11): 5053
- 14 Al-Hussein M, Schindler M, Ruderer M A et al. *Langmuir*[J], 2013, 29(8): 2490
- 15 Hussain A, Pu H, Sun D. *Spectrochimica Acta Part A: Molecular and Biomolecular Spectroscopy*[J], 2020, 229: 117 994
- 16 Miyamoto D, Oishi M, Kojima K et al. *Langmuir*[J], 2008, 24(9): 5010
- 17 Penn R L, Banfield J F. *Science*[J], 1998, 281(5379): 969
- 18 Kan C, Zhu X, Wang G. *The Journal of Physical Chemistry B*[J], 2006, 110(10): 4651
- 19 Pardinas-Blanco I, Hoppe C E, Pineiro-Redondo Y et al. *Langmuir*[J], 2008, 24(3): 983
- 20 Sun Y, Ye J, Minor A M et al. *Microsc Res Techniq*[J], 2009, 72(3): 232
- 21 Ren Y, Liu J, Feng F et al. *Chinese J Chem*[J], 2011, 29(9): 1955 (in Chinese)
- 22 Jaber S Y S, Ghaffarinejad A. *International Journal of Hydrogen Energy*[J], 2019, 44(57): 29 922
- 23 Huang J, Ma D, Xu K et al. *Rare Metal Materials and Engineering*[J], 2019, 48(6): 1791 (in Chinese)
- 24 Kiely C J, Fink J, Brust M et al. *Nature*[J], 1998, 396(6710): 444
- 25 Pei L, Mori K, Adachi M. *Langmuir*[J], 2004, 20(18): 7837
- 26 Cao X, Chen S, Li W et al. *AIP Advances*[J], 2018, 8(10): 105 133
- 27 Wang C, Kan C, Ni Y et al. *Acta Phys-Chim Sin*[J], 2014, 30(1): 194
- 28 Leopold N, Chiş V, Mircescu N E et al. *Colloids and Surfaces A: Physicochemical and Engineering Aspects*[J], 2013, 436: 133
- 29 Frens G. *Nature*[J], 1973, 241: 20
- 30 Dahal U, Wang Z, Dormidontova E E. *Macromolecules*[J], 2018, 51(15): 5950
- 31 Lin W H, Lu Y H, Hsu Y J. *J Colloid Interf Sci*[J], 2014, 418: 87
- 32 Lu L, Kobayashi A, Kikkawa Y et al. *The Journal of Physical Chemistry B*[J], 2006, 110(46): 23 234
- 33 Liu L, Nakouzi E, Sushko M L et al. *Nature Communications*[J], 2020, 11(1): 1045
- 34 Lofton C, Sigmund W. *Advanced Functional Materials*[J], 2005, 15(7): 1197
- 35 Kan C, Zhu X, Wang G. *The Journal of Physical Chemistry B*[J], 2006, 110(10): 4651
- 36 Yoon Y S, Sohn H S, Lee J C. *Polymer*[J], 2009, 50(6): 1395
- 37 Wang T, Hu X, Wang J et al. *Talanta*[J], 2008, 75(2): 455
- 38 He H, Wu C, Bi C et al. *Chemistry-A European Journal*[J], 2021, 27(27): 7549
- 39 Song W, Wang Y, Zhao B. *Journal of Physical Chemistry C*[J], 2007, 111(34): 12 786
- 40 Yigit N, Velioglu Y S. *Critical Reviews in Food Science and Nutrition*[J], 2020, 60(21): 3622
- 41 Song Y, Zhang Y, Huang Y et al. *Analytical Letters*[J], 2020, 53(7): 1003
- 42 Li X, Zhang S, Yu Z et al. *Appl Spectrosc*[J], 2014, 68(4): 483
- 43 Hou R, Pang S, He L. *Anal Methods*[J], 2015, 7(15): 6325
- 44 GB 2763-2021[S], 2021 (in Chinese)

金多孔纳米片的一锅法制备及其在SERS检测中的应用

王翠萍, 张欢, 吴国强, 洪艳平, 颜贤仔, 余莉莉, 王纯荣

(江西农业大学 食品科学与工程学院, 江西 南昌 330045)

摘要: 设计并构建多样的金微纳米结构是实现表面增强拉曼光谱(SERS)信号放大的合理途径。利用氯金酸与聚乙二醇(PEG)的氧化还原反应,通过水热合成法制备出金多孔纳米片。PEG在制备过程中既是包裹剂又是还原剂。该制备方法反应温度比较温和,采用一锅法一步合成工艺,成本效益高且环境友好。所制备的金多孔片尺寸多为微米级,清洗后表面没有有机物污染。EDS分析进一步证实所制备的多孔片结构为金单质。结果表明,金多孔纳米片的形貌可通过反应时间、PEG浓度和金离子浓度等实验参数进行调整。金多孔纳米片制备的拉曼光谱基底具有优异的SERS光谱增强效果,并在检测中表现出良好的重现性。另外,所制备的金纳米多孔片基底实现了有机农药福美双和甲拌磷的快速灵敏分析检测。

关键词: 金; 多孔纳米片; SERS; 聚乙二醇

作者简介: 王翠萍,女,1995年生,硕士,江西农业大学食品科学与工程学院,江西 南昌 330045, E-mail: cpwang2020@163.com